さまざまなシグナル経路が関与している．DTXを含む多くの抗がん剤に対する多剤耐性の分子機構として，adenosine triphosphate binding cassette (ABC) transportersの過剰発現がある．ABC transportersは，イオンやタンパク質といった多様な物質の輸送に関連する膜タンパク質の一群で，多くの組織や細胞に存在し有害物質の排出ポンプとして機能している．ヒトにおいては約50種類のABC transportersが確認され，4つのサブファミリーに分類される．ABC transportersの一つであるP-glycoprotein (P-gp)は，見かけ上130～180 kDaの分子量で，ATPを介して毒性物質を細胞外へ排出する．P-gpは，正常な前立腺組織において発現が低い一方で，前立腺腫瘍上皮で発現が高いことが認められ，前立腺がん細胞において，P-gpの発現量が薬剤抵抗性と相関することも報告されている[6]．また，同じくABC transportersのBCRP/ABCG2は，serine/threonine kinaseの一つであるPim-1にリン酸化されることで，前立腺がん細胞株においてDTX抵抗性を示すことが認められた[7]．

抗がん剤抵抗性には，Nuclear factor for κ-kinase gene in B cells (NF-κB) シグナル経路も関与している．NF-κBは，ストレスやサイトカイン等の刺激によって活性化され，細胞増殖やapoptosisなどの細胞死に関与する重要な転写因子である．NF-κBの活性制御不良が，関節リウマチなどの炎症性疾患や癌，敗血症性ショックなどの原因となる．多くのがんにおいて，NF-κBの恒常的活性化が認められることから，NF-κBを阻害することによる抗がん剤感受性の増大が期待される．前立腺がん細胞においては，アンドロゲン依存性のLNCaPやLAPC-4細胞はNF-κBの活性が低い一方で，アンドロゲン非依存性のDU-145やPC-3細胞は，恒常的に活性化していることから，前立腺がんの悪性化にNF-κBが関与していることが示唆される[8]．さらに，臨床検体および細胞株を用いた実験により，DTX投与がNF-κBの活性化を誘導することや，NF-κB遺伝子の発現抑制下で，DTXを投与すると抗腫瘍効果の増大が認められたため，NF-κBの活性化がDTX抵抗性を促進していることが示唆された．このとき，DTX投与によって，炎症性サイトカインの一つであるInterleukin-6 (IL-6)の発現量に変化は認められなかったが，IL-6遺伝子をRNA干渉によって抑制すると，DTXの抗腫瘍効果が増大した[9]．この結果から，IL-6は前立腺がんの薬剤耐性マーカーとなりうると考えられるが，その機能や下流については，更なる解析が必要である．

近年では，DU145やPC-3において，主に細胞増殖の調節，分化に関与するTGF-β superfamilyの一つであるTGF β1が，DTX抵抗性を生じる機能を有することが*in vitro*実験系で示唆された[10]．さらに，DTX抵抗性前立腺がん細胞の生存が，Notch/hedgehog pathwayに依存し，これら経路の阻害剤とDTXを併用することで抗腫瘍効果が増大することが*in vitro*および*in vivo*の実験系で報告されている[11]．これらさまざまなシグナル経路が関与することで，がん細胞は抗がん剤抵抗性を獲得していると考えられる．

3．PI3K/Akt/mTOR signaling

抗がん剤抵抗性に関与するシグナル経路の一つとして，Phosphoinositide-3kinase (PI3K)/Akt/mammalian target of rapamycin (mTOR)が注目されている．PI3Kは上皮細胞増殖因子(Epidermal growth factor：EGF)などの増殖因子によって活性化され，下流に細胞の増殖や細胞分裂に関与する遺伝子群が存在する．mTORは289 kDaのserine/threonine kinaseで，PI3Kの触媒ドメインと非常に良く似た構造を持つことから，PI3K related kinase (PIKK) familyの一つとされ，この構造は酵母からラット，マウス，そしてヒトに至るまで幅広く保存されている．mTORはPI3Kの下流に存在し，ribosomal p70S6K (S6K1)あるいは，eukaryotic initiation factor binding proteins (4E-BP)を直接活性化することで，細胞分裂を促進する．この経路は，さまざまな増殖因子によってPI3Kが活性化することにより，PIP3を生成する．PIP3はこの経路の重要なセカンドメッセンジャーであるAktに直接結合し，その後別のkinaseによりAktが活性化状態となる．この活性化Aktがtuberous sclerosis complex 1 (TSC1)/TSC2複合体を抑制することで，mTORが活性化される．また，TSC1/TSC2複合体を介さずに，Aktは直接mTORをリン酸化し活性化状態にする経路も存在する．哺乳類のmTORは，mTORC1とmTORC2と呼ばれる機能的に異なる二つの複合体を形成する．mTORC1は，Regulatory associated protein of mTOR (RAPTOR)という三つのタンパク質から構成され，栄養物に応答して翻訳や細胞成長を幅広く調節する．mTORC2は，mTOR，mLST8，Rapamycin-insensitive companion of mTOR (RICTOR)，SAPK-interacting protein (SIN1)，Protein-observed with RICTOR-1 (Protor-1)から成る複合体を形成し，アクチン細胞骨格ダイナミクスを調節する．mTORC1，mTORC2どちらの複合体もAktによって直接活性化される．Aktが，このような複合体を始めとするさまざまな生存促進や成長促進を行うための標的分子をリン酸化することで，生体内では造腫瘍効果を持つことが示唆されている(図1)[12,13]．

この経路を負に制御するがん抑制遺伝子が，染色体上の10q23.3に位置しているPhosphatase and tensin homolog (PTEN)である．PTENはPIP3を脱リン酸化することにより，下流のAktやmTORを抑制している．しかし，多くのがんで，PTEN遺伝子は片アリル欠損やメチル化などのエピジェネティック修飾による，PTENタンパク質の機能欠損が報告され，予後との相関も認められている[14]．前立腺がんにおいては，約80%に同タンパク質の機能損失が認められ，PTEN欠損マウスモデルによって前立腺がんが進行することも認められ[15]，前立腺がんの治療において，PI3K/Akt/mTOR signaling経路は非常に密接に関与していると考えられる．

4．前立腺がんに対して使用される抗がん剤の作用機序

4．1　ドセタキセル

ドセタキセル(DTX)は，微小管タンパクの脱重合を阻害することにより微小管の安定化，過剰形成を促進し，細胞分裂を阻害することや，Bcl-2のリン酸化およびCaspase-3の活性化を誘導することで，抗腫瘍効果を発揮すると考えられている．当研究室では，再燃前立腺がんに対する化学療法のFirst lineとして使用されるDTXと，磁性体ナノ粒子の一つであるマグネタイト(Fe_3O_4)を前立腺がん細胞株に併用曝露することで，より少ないDTXの量で，効果が維持できることを以前報告した．

4．2　Rapamycin

Rapamycinは，南太平洋の島であるRapa Nuiの土壌サンプルから分離された，マクロライド系天然抗生物質である．RapamycinはFK506と呼ばれる免疫抑制剤と構造が似ていて，mTORを標的としている．近年，ヒトのがんだけでなく，2型糖尿病のような代謝不全や，造腫瘍症候群においてmTORに制御異常が認められたことから，非常に注目されている抗腫瘍薬の一つである．Rapamycinは狭心症におけるステント治療後の冠動脈再狭窄を抑制するための薬として使用されるが，中性脂肪の増加や，血小板の減少といった副作用も生じる．Rapamycinは，細胞内レセプターのFK506 binding protein (FKBP12)と複合体を形成し，この複合体がmTORのkinase活性を阻害する．mTORがRapamycinによって阻害された結

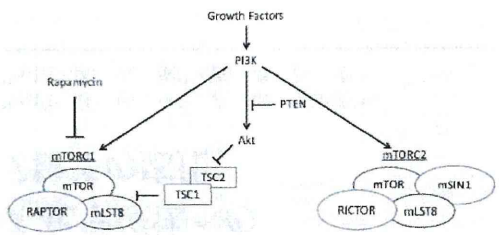

図1　PI3K/Akt/mTOR signaling経路

果，細胞周期のG1期で増殖停止され，G0期と同様にタンパク質合成も停止する．Rapamycinと良く似たmTOR阻害剤として，temsirolimus，everolimus，ridaforolimusやdeforolimus由来の物質が，さまざまながんに対応する抗がん剤として開発されている．

4．3　カルボプラチン(Carboplatin)

現在，がん化学療法の中心的な役割を担う抗がん剤がプラチナ製剤で，精巣腫瘍や卵巣がんを始めとする，数多くのがん種に対して有効性が認められている．プラチナ製剤は，DNAに直接作用する抗がん剤で，体内で活性体に変換後，がん細胞内のDNAやタンパク質に結合することにより，DNAの複製および転写を阻害し，死滅させる．代表的なプラチナ製剤はシスプラチンで，高い抗腫瘍効果を有するが，腎障害や骨髄抑制といった激しい副作用が生じ易い．そこで，シスプラチンの抗腫瘍効果を弱めることなく，かつ腎毒性などの副作用を軽減することを目的に開発されたプラチナ製剤が，カルボプラチンである．当研究室では，前立腺がん細胞株DU145にカルボプラチンを投与後，48，72時間後に細胞生存率をAlamar blue assayによって測定した結果，濃度依存的に細胞生存率が減少することが観察された(図2)．また，本邦で前立腺がん治療に良く用いられたエストラムスチン(EMP)とDTX，カルボプラチンを併用投与すると，前立腺がん患者のPSA値が30％以上低下する臨床試験結果も報告されている[16]．従って，今後，カルボプラチンは，前立腺がんに対するSecond lineとして有望視されている．

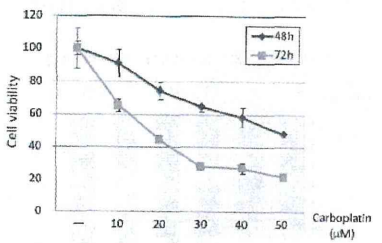

図2　Carboplatin投与時における DU145 の細胞生存率

5．前立腺がん細胞における磁性体ナノ粒子の影響

近年，ナノテクノロジーは，がんを始めとする医療分野への応用が注目されている．ナノ粒子は，難溶性の薬剤の輸送や，標的組織あるいは器官への薬物輸送，診断薬や薬剤との併用による効果増強などが期待できる．そのためには，ナノ粒子の特徴を理解した上で，従来の治療法を改善していく必要がある．超常磁性体酸化金属ナノ粒子(Superparamagnetic iron oxide nanoparticles：SPION)は，機能性材料として注目され，その特徴を活かして，磁気共鳴装置(Magnetic resonance imaging：MRI)の造影剤，薬剤や遺伝子を目的の臓器へ輸送するシステム(Drug delivery system：DDS)，温熱療法(Hyperthermia)，キレート療法などに応用されている[17,18]．

SPIONの一つであるマグネタイトナノ粒子(Fe_3O_4-NP)は，他のナノ粒子と比べて高い生体適合性を有し，細胞内に浸透しやすいことから[19]，医療分野，特にがんに対する治療法や診断法の応用に向けて，盛んに研究されている．当研究室では，以前Fe_3O_4-NPのヒト細胞株（肺がん細胞株A549，前立腺がん細胞株LNCaP，DU145，PC-3，前立腺上皮細胞RWPE-1など）への細胞毒性および遺伝毒性の評価を行ってきた．その結果，Fe_3O_4-NP曝露による前立腺がん細胞株に濃度依存的な細胞生存率の低下，および酸化ストレスの指標となる8-hydroxydeoxyguanosine(8-OH-dG)の有意な増加が認められた．このことから，Fe_3O_4-NPは，前立腺がん細胞株に対して，細胞毒性および遺伝毒性を生じさせると考えられた．その後，Fe_3O_4-NPは，前立腺がん細胞株に活性酸素種(Reactive Oxygen Species：ROS)を増加させるという結果が得られた．Fe_3O_4-NPは，Fenton反応($H_2O_2 + Fe^{2+} \rightarrow Fe^{3+} + HO^- + HO^*$)により生成するフリーラジカルによって，酸化ストレスが生じることが報告されている．マウスのマクロファージ細胞にFe_3O_4-NPを曝露すると，ROSが生じ，そのROSが細胞死を誘導することが報告されているため[20]，前立腺がん細胞株に対しても，ROS産生が上昇することにより，細胞毒性や遺伝毒性が生じると考えられた．

ROS自体はsecond messengerとして正常細胞のシグナリングで重要な役割を果たしている．化学療法，放射線療法および光線力学的治療法においてROSの産生が細胞死をもたらす重要な役割を果たしている．そこで，ROSを産生することで，抗腫瘍効果を誘発する酸化促進がん療法(Pro-oxidant therapy)が考えられている．一般的に，酸化促進がん療法は，ArsenicやImexon等によるROS産生，Glutathione(GSH)の消耗などが該当する．本研究室は，Fe_3O_4-NPによって生じるROS産生を酸化促進がん療法として応用可能であると考えた．つまり，各種抗がん剤とFe_3O_4-NPをがん細胞に併用曝露することで，抗がん剤の抗腫瘍効果を弱めることなく，抗がん剤の使用量を減少させ，副作用を軽減することが可能となると考えられる．

6．RapamycinとFe_3O_4-NPの併用効果

当研究室では，前立腺がん細胞株にfirst lineで使用されるDTXとFe_3O_4-NPを併用曝露し，DTXの使用量を減らし，その効果が維持できることを報告している[21]．また，前立腺がんにおいてPI3K/Akt/mTORsignaling経路は重要な働きをすることが知られている．そこで，現在PI3KやmTORを標的にした多くの分子標的治療薬の開発が進められており，それらの抗腫瘍効果が報告されている(表1)．mTORはmTOR complex 1(mTORC1)と，mTOR complex 2(mTORC2)から

表1　PI3K/Akt/mTOR経路標的薬剤の臨床試験[12]

Drug category	Drug or agent name	Company	Phase of clinical trials	Cancer type
Pan-PI3K inhibitors	GSK1059615	GlaxoSmithKline	Phase I terminated	Solid tumors; metastatic breast cancer endometrial cancer and lymphoma
	ZSTK474	Zenyaku Kogyo Co, Ltd	Phase I	Advanced solid malignancies
	CH5132799	Chugai Pharma Europe Ltd	Phase I	Advanced solid malignancies
Selective PI3K inhibitors	BKM120	Novartis	Phase I – II	Solid tumors
	XL147	Exelixis	Phase I – II	lymphoma; breast cancer; endometrial cancer; NSCLC; ovarian cancer; glioblastoma; astrocytoma
	GDC0941	Genentech	Phase I	Advanced solid tumors; non-Hodgkin's lymphoma; locally recurrent breast cancer; metastatic breast cancer; NSCLC
	PX866	Oncothyreon, Inc.	Phase I – II	Incurable metastatic colorectal carcinoma; incurable progressive, recurrent, or metastatic squamous cell carcinoma of the head and neck; advanced solid tumor; prostate cancer; glioblastoma
PI3K (α isoform)	BYL719	Novartis	Phase I	Advanced solid tumors with a mutation of the PIK3CA gene
PI3K (δ isoform)	CAL-101	Calistoga	Phase I – II	Non-Hodgkin's lymphoma; chronic lymphocytic leukemia; small lymphocytic lymphoma; acute myeloid leukemia; multiple myeloma; allergic rhinitis
Akt Inhibitors	Perifosine	Keryx	Phase I – III	NSCLC; solid tumors; metastatic breast cancer; sarcoma; childhood solid tumors; malignant gliomas; lymphomas; colon cancer; multiple myeloma; solid tumors
	MK-2206	Merck	Phase I – II	Advanced solid tumors; breast cancer; lymphoma; colorectal neoplasms; leukemia; ovarian cancer; fallopian tube cancer
	GSK690693	GlaxoSmithKline	Phase I (terminated)	Relapsed or refractory hematologic malignancies; solid tumors; lymphoma
mTOR Kinase Inhibitors	AZD8055	AstraZeneca	Phase I – II	Advanced solid malignancies; glioblastoma multiforme; anaplastic astrocytoma; anaplastic oligodendroglioma; malignant glioma; brainstem glioma; advanced hepatocellular carcinoma
	OSI027	OSI Pharmaceuticals	Phase I	Solid tumors; lymphoma
	INK-128	Intellikine	Phase I	Breast cancer; advanced solid malignancies; non-Hodgkin's lymphoma; relapsed or refractory multiple myeloma
Rapamycin and Rapamycin Analogues (Rapalogues)	Rapamycin	Wyeth/Pfizer	Phase I – II	Glioma; renal cell carcinoma; advanced solid cancers; bladder cancer; head and neck cancer; renal cell carcinoma
	Temsirolimus	Wyeth/Pfizer	Phase I – III	Metastatic cancers; advanced solid tumors; breast cancer; glioma; NSCLC; renal cell carcinoma; head and neck cancer; bladder cancer; colorectal cancer; thyroid cancer; squamous cell cancer; prostate cancer; non-Hodgkin's lymphoma; multiple myeloma; malignant melanoma; endometrial cancer; ovarian cancer; glioblastoma multiforme; sarcoma
	Everolimus	Novartis	Phase I – III	Bladder cancer; advanced solid tumor; head and neck cancer; gliomas; renal cell carcinoma; lymphoma; kidney cancer; endometrial cancer;

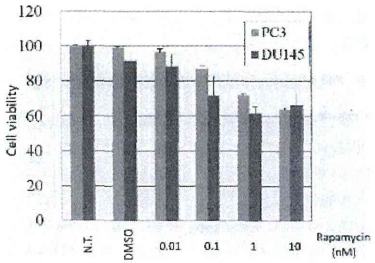

図3　Rapamycin 投与から 72 時間後の細胞生存率

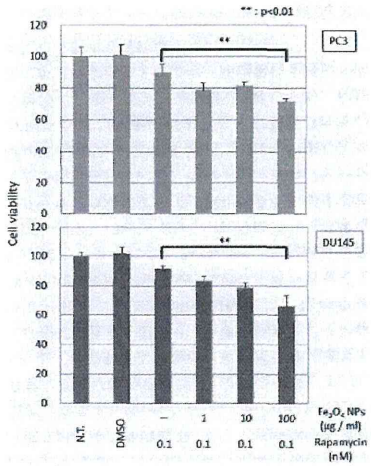

図4　Rapamycin と Fe_3O_4-NP 併用曝露後の細胞生存率

なる複合体を形成する．そして，マクロライド系抗生剤であり，前立腺がん治療の Second line として有望視されている Rapamycin により mTORC1 が特異的に阻害される．しかし，PI3K/Akt/mTOR シグナル経路は，PTEN により制御されているので，PTEN の有無により Rapamycin の効果が異なると考えられるため，二つの前立腺がん細胞株 DU145（PTEN 陽性）および PC-3（PTEN 欠損）に対して，Rapamycin を曝露し，72 時間後の細胞生存率を測定した．その結果，DU145，PC-3 細胞株共に濃度依存的に細胞生存率が減少した（図3）．Rapamycin は，がん抑制遺伝子である PTEN や TP53 遺伝子が機能損失しているがん細胞に対して有効性が認められている[14]．DU145 細胞株は，PTEN 陽性であるが，TP53 に変異を有する細胞株であるため，この細胞株において Rapamycin が細胞生存率に影響を与えたことが考えられる．実際，別の PI3K/Akt/mTOR シグナル経路阻害剤 BEZ235 を DU145，PC-3 両細胞株に曝露しても，両細胞株共に細胞生存率の低下が認められている[22]．次に，両細胞株に対して，Rapamycin と Fe_3O_4-NP の併用曝露を行った結果，通常使用される Rapamycin の 1/100 量（0.1 nM）を使用したにもかかわらず，Fe_3O_4-NP 濃度依存的に細胞生存率の低下が認められた．さらに，Rapamycin（0.1 nM）と Fe_3O_4-NP 100 μg/ml 曝露条件下において，Rapamycin（0.1 nM）単剤よりも統計学的に有意に細胞生存率が減少する結果が得られた（図4）．Fe_3O_4-NP を用いた併用療法に対する研究は数多く存在し，作用機序もさまざまである．例えば，大腸がん細胞株 LOVO に対しては，Fe_3O_4-NP と *Gambogic acid* を併用曝露すると，PI3K/Akt/Bad シグナル経路を介して，細胞増殖を抑制する[23]．また，白血病マウスモデルにおいては，Fe_3O_4-NP と抗がん剤の Daunoru-bicin，5-bromotetrandrine を併用投与すると，apoptosis 経路が活性化して細胞死を誘導することが報告されている[24]．当研究室で DTX と Fe_3O_4-NP を併用曝露した際，ROS の産生が向上し，apoptosis の割合が増加したことから，Rapamycin と Fe_3O_4-NP の併用曝露においても酸化ストレスが向上している可能性がある．そこで，Rapamycin と Fe_3O_4-NP の併用によって生じる細胞死は，さまざまな経路が関与していることが考えられるので，今後，さらに詳細な生物学的機構の解析が必要となる．

7．まとめ

前立腺がんの治療に対する FDA 承認薬は，2004 年の DTX 以降現在に至るまで，Cabazitaxel，Abiraterone，Sipuleucel-T の 3 つがある．さらに，第 3 相臨床試験の最新の結果によれば，MDV 3100 と Alpharadin という試験薬が，前立腺がん男性の全生存期間を改善することが報告され，さらに二つ加わる可能性がある．PI3K/Akt/mTOR シグナル経路に関する薬剤としては，mTOR/PI3K 複数個所同時に阻害する薬剤が，いくつか臨床試験に進んでいることから，前立腺がんに対する治療薬の選択肢が今後増加していくことが予想される．一方で，Gold nanoparticles（Au-NP）や Fullerenes（C_{60}），Carbon Black（CB）などの別のナノ粒子と抗がん剤を併用する実験も行われている．前立腺がんにおいては，Au-NP と前立腺特異的膜抗原（Prostate-specific membrane antigen：PSMA）阻害剤を併用することで，細胞生存率が低下することが報告されている[25,26]．また，Fe_3O_4-NP を物質でコーティングした修飾ナノ粒子を治療分野に応用する研究も行なわれている．例えば，dextran 修飾 Fe_3O_4-NP は，肝臓，脾臓，肺に蓄積しやすく，*Angelica* polysaccharide 修飾 Fe_3O_4-NP は脾臓と肺にしか蓄積しないなど，標的臓器への薬剤輸送を目的とした研究がなされている[27]．現在，当研究室でも，カルボキシル基や，ポリエチレンイミン（Polyethyleneimine：PEI），界面活性剤の pluronic などを修飾した Fe_3O_4-NP を用いて，研究を行っている．従って，今後，抗がん剤とナノ粒子の両方面で研究を進めていくことで，前立腺がんの治療法改善が期待できると思われる．

参考文献

1）Tabata, N., *et al.*, *Jpn J Clin Oncol*, 2008. **38**(2)：p.146-57.
2）Watanabe, M., *et al.*, *Urol Oncol*, 2000. **5**(6)：p.274-283.
3）Colloca, G., A. Venturino, and F. Checcaglini, *Med Oncol*, 2012. **29**(2)：p.776-85.
4）Kao, S.C., E. Hovey, and G. Marx, *Asia Pac J Clin Oncol*, 2011. **7**(3)：p.212-23.
5）Hwang, C., *Ther Adv Med Oncol*, 2012. **4**(6)：p.329-40.
6）Sanchez, C., *et al.*, *Prostate*, 2009. **69**(13)：p.1448-59.
7）Xie, Y., *et al.*, *J Biol Chem*, 2008. **283**(6)：p.3349-56.
8）Mahon, K.L., *et al.*, *Endocr Relat Cancer*, 2011. **18**(4)：p.R103-23.
9）Codony-Servat, J., *et al.*, Prostate, 2012.
10）Marin-Aguilera, M., *et al.*, *Mol Cancer Ther*, 2012. **11**(2)：p.329-39.
11）Domingo-Domenech, J., *et al.*, *Cancer Cell*, 2012. **22**(3)：p.373-88.
12）Bartholomeusz, C. and A.M. Gonzalez-Angulo, *Expert Opin Ther Targets*, 2012. **16**(1)：p.121-30.
13）Zaytseva, Y.Y., *et al.*, *Cancer Lett*, 2012. **319**(1)：p.1-7.
14）Rai, J.S., M.J. Henley, and H.L. Ratan, *Urol Oncol*, 2010. **28**(2)：p.134-8.
15）Floc'h, N., *et al.*, *Cancer Res*, 2012. **72**(17)：p.4483-93.
16）Yasufuku, T., *et al.*, *J Infect Chemother*, 2010. **16**(3)：p.200-5.
17）Singh, N., *et al.*, *Nano Rev*, 2010. 1.
18）Sanna, V. and M. Sechi, Nanomedicine, 2012. 8 Suppl 1：p.S31-6.
19）Jain, K.K., *BMC Med*, 2010. **8**：p.83.
20）Naqvi, S., *et al.*, *Int J Nanomedicine*, 2010. **5**：p.983-9.
21）一町直樹，栗岡大輔，河合一明，邑西　宏，松本幹治，渡邉昌俊，粉体工学会誌，2011. **48**：p.145-151
22）Potiron, V.A., *et al.*, Radiother Oncol, 2013.
23）Fang, L., *et al.*, *Int J Nanomedicine*, 2012. **7**：p.4109-18.
24）Ren, Y., *et al.*, Int J Nanomedicine, 2012. **7**：p.2261-9.
25）Kasten, B.B., *et al.*, *Bioorg Med Chem Lett*, 2013. **23**(2)：p.565-8.
26）Dreaden, E.C., *et al.*, *Bioconjug Chem*, 2012. **23**(8)：p.1507-12.
27）Wang, L., *et al.*, *J Huazhong Univ Sci Technolog Med Sci*, 2012. **32**(3)：p.444-50.

International Journal of Nanomedicine

Dovepress

ORIGINAL RESEARCH

Magnetic nanoparticles of Fe_3O_4 enhance docetaxel-induced prostate cancer cell death

Akiko Sato[1]
Naoki Itcho[1]
Hitoshi Ishiguro[2,3]
Daiki Okamoto[1]
Naohito Kobayashi[4]
Kazuaki Kawai[5]
Hiroshi Kasai[5]
Daisuke Kurioka[1]
Hiroji Uemura[2]
Yoshinobu Kubota[2]
Masatoshi Watanabe[1]

[1]Laboratory for Medical Engineering, Division of Materials Science and Chemical Engineering, Graduate School of Engineering, Yokohama National University, Yokohama, Japan; [2]Department of Urology, Yokohama City University Graduate School of Medicine, Yokohama, Japan; [3]Photocatalyst Group, Kanagawa Academy of Science and Technology, Kawasaki, Japan; [4]Department of Molecular Pathology, Yokohama City University Graduate School of Medicine, Yokohama, Japan; [5]Department of Environmental Oncology, Institute of Industrial Ecological Sciences, University of Occupational and Environmental Health, Kitakyushu, Japan

Correspondence: Masatoshi Watanabe
Laboratory for Medical Engineering, Division of Materials Science and Chemical Engineering, Graduate School of Engineering, Yokohama National University, 79-5 Tokiwadai, Hodogayaku, Yokohama, Japan
Tel +81 453 393 997
Fax +81 453 393 997
Email mawata@ynu.ac.jp

Abstract: Docetaxel (DTX) is one of the most important anticancer drugs; however, the severity of its adverse effects detracts from its practical use in the clinic. Magnetic nanoparticles of Fe_3O_4 (MgNPs-Fe_3O_4) can enhance the delivery and efficacy of anticancer drugs. We investigated the effects of MgNPs-Fe_3O_4 or DTX alone, and in combination with prostate cancer cell growth in vitro, as well as with the mechanism underlying the cytotoxic effects. MgNPs-Fe_3O_4 caused dose-dependent increases in reactive oxygen species levels in DU145, PC-3, and LNCaP cells; 8-hydroxydeoxyguanosine levels were also elevated. MgNPs-Fe_3O_4 alone reduced the viability of LNCaP and PC-3 cells; however, MgNPs-Fe_3O_4 enhanced the cytotoxic effect of a low dose of DTX in all three cell lines. MgNPs-Fe_3O_4 also augmented the percentage of DU145 cells undergoing apoptosis following treatment with low dose DTX. Expression of nuclear transcription factor κB in DU145 was not affected by MgNPs-Fe_3O_4 or DTX alone; however, combined treatment suppressed nuclear transcription factor κB expression. These findings offer the possibility that MgNPs-Fe_3O_4–low dose DTX combination therapy may be effective in treating prostate cancer with limited adverse effects.

Keywords: prostate cancer, magnetic nanoparticles, docetaxel, reactive oxidative species

Introduction

Prostate cancer is the most common cancer affecting men, and the second leading cause of cancer death in the United States.[1] The incidence and mortality rates of prostate cancer vary greatly among different geographic areas and ethnic groups. Although the incidence of prostate cancer in Japan remains low compared with that in the United States, it has been increasing in recent years. However, by 2020, prostate cancer is projected to surpass stomach cancer as the most frequently diagnosed cancer in Japanese men.[2]

Several management options are available when prostate cancer is diagnosed at an early stage, including watchful waiting, surgery, cryosurgery, radiation therapy, and hormonal therapy. For advanced prostate cancers, surgical or medical ablation of androgens is regarded the optimal first-line treatment. In most patients treated by androgen deprivation, disease progression will continue until reaching a stage referred to as castration-resistant prostate cancer (CRPC). Progression to a hormonal refractory state is a complex process, involving both selection and outgrowth of preexisting clones of androgen-independent cells as well as adaptive upregulation of genes that help cancer cells survive and grow after androgen ablation.[3]

Although the effects of several anticancer drugs for prostate cancer have been evaluated in vitro and in animal experiments in vivo, most have little or no impact

on the survival of patients with CRPC or metastatic prostate cancer.[4,5] Docetaxel (DTX), a semisynthetic toxoid produced from the needles of the European yew tree, is the first chemotherapy agent to improve survival in CRPC, and the US Food and Drug Administration has recommended a 3-week DTX-prednisone regimen as a first-line treatment option for CRPC patients.[6–8] Although DTX-based chemotherapy may provide some benefits, most CRPC patients do not realize them, and the average survival remains relatively brief. Moreover, the current regimen requires the administration of high doses of DTX, which causes toxic reactions and thereby precludes the use of DTX as a monotherapy.[9] To reduce toxicity and to improve the survival and quality of life of CRPC patients, novel therapeutic strategies targeting the molecular basis of androgen- and chemo-resistance of prostate cancer using a reduced but equieffective dose of DTX should be developed.

Cancer nanotechnology offers great potential for cancer diagnosis, targeted treatment, and monitoring.[10] Researchers are exploring the use of nanoparticles (NPs) ranging in length from 1 nm to 100 nm in two or three dimensions to detect, image, monitor, and treat cancers. Among the rapidly evolving types of NPs, magnetic NPs (MgNPs) – biocompatible and superparamagnetic nanomaterials with chemical stability and low toxicity – are especially promising.[11] The combination of MgNPs with anticancer agents has been applied to leukemia, lung, and pancreatic cancer cells in vitro and to xenograft-injected nude mice.[12–15] MgNPs composed of Fe_3O_4 (MgNPs-Fe_3O_4) are being widely investigated for use as targeted drug carriers. The aim of this study was to evaluate the effect of treatment with MgNPs-Fe_3O_4 or MgNPs-Fe_3O_4 combined with DTX on prostate cancer cell growth in vitro. We also explored the mechanism underlying MgNPs-Fe_3O_4-induced cell death, focusing on the effect of MgNPs-Fe_3O_4 treatment on the production of reactive oxygen species (ROS).

Materials and methods

Physical characterization of MgNPs-Fe_3O_4

MgNPs-Fe_3O_4 were obtained from the Toda Kogyo Corporation (Otake, Hiroshima, Japan) and had the following characteristics: spherical shape; an average particle size of 10 nm in powder and 8–10 nm as measured by transmission electron microscopy (TEM); a size of 60–100 nm as measured by dynamic light scattering (DLS); a zeta potential of −30 to −40 mV at a pH of 10; and a surface area in powder of 100–120 m^2/g.

Preparation of MgNPs-Fe_3O_4

After ultraviolet sterilization of the particles, MgNPs-Fe_3O_4 stocks were prepared by suspending particles in Roswell Park Memorial Institute (RPMI)-1640 with supplements to yield final concentrations of 1 μg/mL, 10 μg/mL, or 100 μg/mL, followed by sonication at 30 W for 10 minutes with an Ultrasonic Homogenizer VP-050 (TAITEC, Koshigaya, Saitama, Japan).

Docetaxel

DTX was purchased from Sigma-Aldrich (St Louis, MO, USA) and dissolved in dimethyl sulfoxide (DMSO; stock solution). Stock solutions were aliquoted and stored at −20°C to avoid repetitive freeze–thaw cycles. Stock solutions were serially diluted using culture medium to prepare working solutions.

Cell lines

LNCaP, DU145, and PC-3 human prostate cancer cell lines were purchased from American Tissue Type Culture Collection (Manassas, VA, USA). Cells were cultured in RPMI-1640 medium with 10% fetal bovine serum (FBS) and 100 U/mL penicillin–streptomycin in 5% CO_2 at 37°C. The human normal prostate stromal cell (PrSC) line was obtained from BioWhittaker® (Lonza Walkersville, Inc, Walkersville, MD, USA) and maintained in Dulbecco's modified Eagle's medium supplemented with 10% FBS, 100 U/mL of penicillin G, 100 μg/mL of streptomycin, ITH (5 μg/mL insulin, 5 μg/mL transferrin, and 1.4 μmol/L hydrocortisone), and 5 ng/mL of bFGF in 5% CO_2 at 37°C.

Characterization of MgNPs-Fe_3O_4 suspension

MgNP-Fe_3O_4 suspensions and their cellular localization were characterized using the following methods.

Dynamic light scattering (DLS)

The average hydrodynamic size and size distribution of MgNPs-Fe_3O_4 in media were determined by DLS using a Fiber-Optics Particle Analyzer FPAR-1000 (Otsuka Electronics Co, Ltd, Hirakata, Osaka, Japan). DU145 cells were incubated with MgNPs-Fe_3O_4 (1 μg/mL, 10 μg/mL, or 100 μg/mL).

Transmission electron microscopy (TEM)

DU145 cells were incubated with MgNPs-Fe_3O_4 (10 μg/mL). After incubation for 24 hours, cells were collected, washed three times with phosphate buffered saline (PBS), and fixed

with 3% glutaraldehyde in 0.1 M cacodylate buffer (pH 7.3) at 4°C for 4 hours. The resulting samples were postfixed with 2% osmium tetraoxide at 4°C for 2 hours, dehydrated, and embedded in epoxy resin. Ultrathin sections (80 nm) were then stained with uranyl acetate and lead citrate, and observed by TEM.

Measurement of intracellular reactive oxygen species

ROS were measured using the CM-H2DCFDA assay (Life Technologies, Carlsbad, CA, USA), according to the manufacturer's instructions. DU145 cells (1.0×10^5 cells/well) were incubated with MgNPs-Fe_3O_4 (1 μg/mL, 10 μg/mL, or 100 μg/mL) for 24 hours in the absence or presence of N-acetylcysteine (NAC; 10 mM) (Sigma-Aldrich Co); NAC was added 3 hours before treatment with MgNPs-Fe_3O_4. A stock solution of CM-H2DCFDA (5 mM) was freshly prepared in DMSO and diluted to a final concentration of 1 μM in PBS. Cells were washed with PBS followed by incubation with 50 μL of working solution of fluorochrome marker CM-H2 DCFDA for 30 minutes. Fluorescent imaging was recorded using an IX2 N-FL-1 microscope (Olympus Corporation, Tokyo, Japan), and analyzed using imaging software (Adobe Photoshop Elements 8; Adobe Systems Incorporated, San Jose, CA, USA). As a positive control, cells were treated with H_2O_2 (100 μM) for 24 hours.

Analysis of 8-hydroxydeoxyguanosine in DNA

The MgNPs-Fe_3O_4 (1 μg/mL, 10 μg/mL, or 100 μg/mL) were added to wells containing DU145, PC-3, or LNCap cells (5.0×10^6 cells), and incubated for 72 hours at 37°C (5% CO_2). Nuclear deoxyribonucleic acid (DNA) of the cells was isolated by the sodium iodide method. Analysis of 8-hydroxydeoxyguanosine (8-OH-dG) was performed as previously described.[16] The 8-OH-dG levels were measured by high performance liquid chromatography electrochemical detection. The amount of 8-OH-dG in the DNA was determined through comparisons with the authentic standards, and expressed as the number of 8-OH-dG per 10^6 deoxyguanosine (dG).

AlamarBlue® assay

Cell viability was determined using the AlamarBlue® assay (Alamar Biosciences, Inc, Sacramento, CA, USA), according to the manufacturer's instructions. Briefly, cells were seeded in 24-well plates (1.0×10^4 cells/well); cells were treated with DTX (0.1 μM, 1 μM, 10 μM, or 100 μM) or DTX (1 nM) plus MgNPs-Fe_3O_4 (1 μg/mL, 10 μg/mL, or 100 μg/mL) for 48 hours at 37°C (5% CO_2). AlamarBlue® was added to each well at 10% volume and was incubated for 200 minutes. Metabolically active cells reduced the dye into a fluorescent form; fluorescence intensity was measured using a plate reader (excitation/emission: 570 nm/600 nm; Viento XS, DS Pharma Biomedical Co, Ltd, Suita, Osaka, Japan). Fluorescence intensity was used to estimate cell viability by linear interpolation between the emission from cells treated with 0.1% saponin (0% viability) and that from untreated cells (100% viability).

Flow cytometry (FCM) analysis for cell apoptosis

The apoptotic peak (sub-G1) of cells was measured using FCM. DU145 cells (1.0×10^6 cells) were seeded in 100 mm culture dishes; cells were either untreated (control), or treated with DTX (1 nM) or MgNPs-Fe_3O_4 (10 μg/mL or 100 μg/mL) in the absence or presence of DTX (1 nM). Aspirated medium was collected to determine the amount of floating cells and cell debris as indicators of cell death. Cells were collected and fixed in ice-cold 70% ethanol and stored at –20°C before use. In preparation for use, cells were washed with PBS and resuspended in PBS before incubation with ribonuclease (0.5 mg/mL) at room temperature for 30 minutes. After the addition of 1 mg/mL of propidium iodide (PI; Sigma-Aldrich), the cells were passed through a 40 mm nylon mesh for analysis using an LSRII flow cytometer (BD Bioscience Franklin Lakes, NJ, USA). The fluorescence intensities of PI were measured by FCM, and the number of cells in the sub-G1 peak was determined. Quantification of the fraction was performed with ModFit LT for Mac 3.0 (Verity Software House, Topsham, ME, USA).

Annexin-V assay was used to detect the early phases of apoptosis. Apoptosis was assessed by monitoring the expression of phosphatidylserine on the outer leaflet – an early marker of apoptotic cell death. Phosphatidylserine was stained with fluorescein isothiocyanate (FITC)-labeled Annexin V. Loss of membrane integrity as a consequence of necrosis was detected using PI staining of DNA. Briefly, DU145 cells (1.0×10^6) were either untreated (control) or treated with DTX (1 nM), or with MgNPs-Fe_3O_4 (10 μg/mL or 100 μg/mL) for 24 hours in the absence or presence of DTX (1 nM). After incubation, cells were harvested, gently washed twice in ice-cold PBS, collected by centrifugation, and then stained using an Annexin V-FITC Kit (Beckman Coulter, Inc, Fullerton, CA, USA) according to the manufacturer's instructions. Cells were then stained with Annexin V and PI for analysis by FCM within 1 hour of staining using the FL1 (FITC) and FL3 (PI) lines.

Western blot analysis

Cells were lysed in Radioimmunoprecipitation assay buffer (Sigma-Aldrich) containing protease inhibitors (Sigma-Aldrich). Total protein concentration was determined by Bio-Rad protein assay reagent (Bio-Rad Laboratories, Hercules, CA, USA). Equal amounts of lysates were resolved on sodium dodecyl sulfate-polyacrylamide gel electrophoresis and transferred to a polyvinylidene fluoride membrane (Merck Millipore, Billerica, MA, USA). Membranes were blocked with a blocking reagent (NOF Corporation, Tokyo, Japan) for 1 hour at room temperature, and incubated overnight at 4°C with the respective primary antibodies in Tris-buffered saline and Tween 20 (TBST). The membranes were washed with TBST three times and incubated with diluted horseradish peroxidase-conjugated secondary antibodies (1:3000 for nuclear factor κB [NFκB]; 1:10,000 for β-actin) for 1 hour at room temperature. After three additional washes, membranes were detected using an enhanced chemiluminescence kit (GE Healthcare UK Ltd, Little Chalfont, UK). Antibodies against NFκB and β-actin were purchased from Santa Cruz Biotechnology, Inc (Santa Cruz, CA, USA) and Sigma-Aldrich, respectively; antirabbit and antimouse horseradish peroxidase-conjugated secondary antibodies were purchased from GE Healthcare (GE Healthcare UK Ltd).

Statistical analysis

All experiments were repeated at least three times. Data are represented as the mean ± standard deviation. Data were analyzed using an unpaired Student's *t*-test with or without Welch's correction and ANOVA. Differences were considered statistically significant at $P < 0.05$.

Results

MgNPs-Fe_3O_4 characterization in cell culture medium

Figure 1 shows the mean hydrodynamic diameter of MgNPs-Fe_3O_4 in medium with supplements as measured by DLS. The mean hydrodynamic diameter of MgNPs-Fe_3O_4 increased with increasing concentration, suggesting that aggregation is enhanced at higher concentrations.

Cellular uptake

Cellular uptake of MgNPs-Fe_3O_4 was evident from TEM microphotographs (Figure 2). MgNPs-Fe_3O_4 were localized within intracellular vesicles.

ROS production

MgNPs-Fe_3O_4 caused dose-dependent increases of ROS production in DU145 and PC-3 cells; a significant increase in LNCaP cells was evident only at the highest dose. Treatment with 100 μg/mL of MgNPs-Fe_3O_4 elicited a

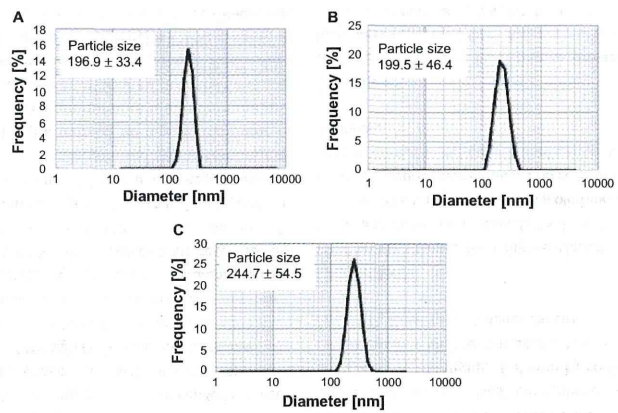

Figure 1 Measurement of MgNPs-Fe_3O_4 size by dynamic light scattering. DU145 cells were incubated with MgNPs-Fe_3O_4: (**A**) 1 μg/mL, (**B**) 10 μg/mL, and (**C**) 100 μg/mL.
Abbreviation: MgNPs-Fe_3O_4, Fe_3O_4 magnetic nanoparticles.

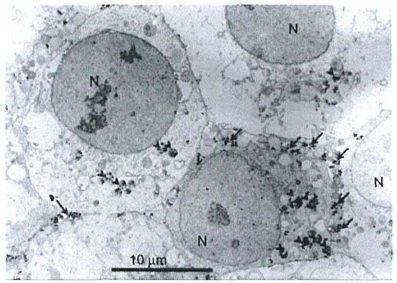

Figure 2 Transmission electron microscopy imaging of DU145 cells treated with 10 µg/mL of Fe_3O_4 magnetic nanoparticles.
Notes: Arrow: extracellular magnetic nanoparticles; arrow head: intracellular magnetic nanoparticles.
Abbreviation: N, nucleus.

response comparable to that evoked by H_2O_2 (Figure 3). Among the three cell lines, ROS levels in the DU145 and PC-3 lines were higher than that in the LNCaP line. Pretreatment with NAC attenuated the MgNPs-Fe_3O_4-induced rise in ROS in all three prostate cancer cell lines (Figure 3).

8-OH-dG levels in DNA

The 8-OH-dG levels in the DNA in all three prostate cancer cell lines increased in a dose-dependent manner (Figure 4). The 8-OH-dG levels of DU145 and PC-3 cells exposed to 10 µg/mL of MgNPs-Fe_3O_4 were 13-fold to 14-fold greater than that of the untreated control cells.

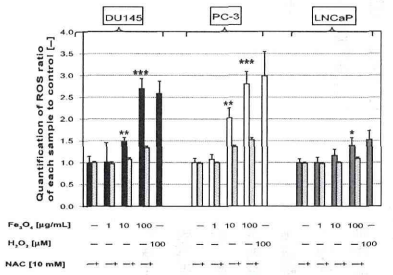

Figure 3 Production of intracellular ROS in DU145, PC-3, and LNCaP cells after treatment with MgNPs-Fe_3O_4 for 24 hours in the absence or presence of NAC.
Notes: Data are presented as the mean ± SD of three independent experiments. *Significantly different from the untreated control at $P < 0.05$; **significantly different from the control at $P < 0.01$; ***significantly different from the untreated control at $P < 0.001$.
Abbreviations: ROS, reactive oxygen species; MgNPs-Fe_3O_4, Fe_3O_4, magnetic nanoparticles; NAC, N-acetylcysteine; SD, standard deviation.

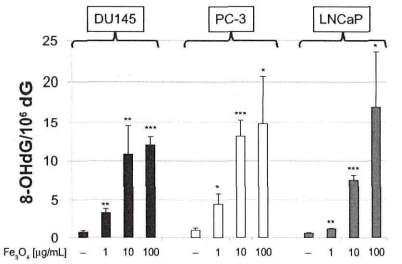

Figure 4 8-OH-dG levels in DU145, PC-3, and LNCaP cells after 72 hours of treatment with MgNPs-Fe_3O_4.
Notes: Data are presented as the mean ± SD of three independent experiments. *Significantly different from the untreated control at $P < 0.05$; **significantly different from the control at $P < 0.01$; ***significantly different from the untreated control at $P < 0.001$.
Abbreviations: 8-OH-dG, 8-hydroxydeoxyguanosine; MgNPs-Fe_3O_4, Fe_3O_4 magnetic nanoparticles; SD, standard deviation.

Effect of MgNPs-Fe_3O_4, DTX, and MgNPs-Fe_3O_4–DTX combinations on cell viability

MgNPs-Fe_3O_4 alone reduced the viability of LNCaP and PC-3 cells, but had little or no effect on the viability of DU145 and PrSC cells (Figure 5). These results suggest that the cytotoxicity of MgNPs-Fe_3O_4 may be dependent on the cell type of the prostate cancer cell line. DTX alone decreased cell viability in a dose-dependent manner in all three cancer cell lines (Figure 6). Combined treatment with MgNPs-Fe_3O_4 and DTX enhanced the inhibitory effect of DTX; in PC-3 cells, 100 µg/mL of MgNPs-Fe_3O_4 plus 1 nM of DTX reduced cell viability so it was similar to that caused by 10 nM DTX alone. These data suggest that MgNPs-Fe_3O_4 may be beneficial in reducing the DTX dose it may and thereby overcome the safety limitations of DTX.

Effect of MgNPs-Fe_3O_4, DTX, and MgNPs-Fe_3O_4–DTX combinations on cell death

An apoptotic fraction of cells containing subdiploid amounts of DNA was detected as a sub-G1 peak (Figure 7). MgNPs-Fe_3O_4 caused a dose-dependent increase in the percentage of DU145 cells in the sub-G1 fraction; similarly, DTX alone elicited a rise in the percentage of cells in the sub-G1 fraction. Combined treatment with MgNPs-Fe_3O_4 plus DTX augmented the effect compared to either treatment alone; this enhancement was dose-dependent.

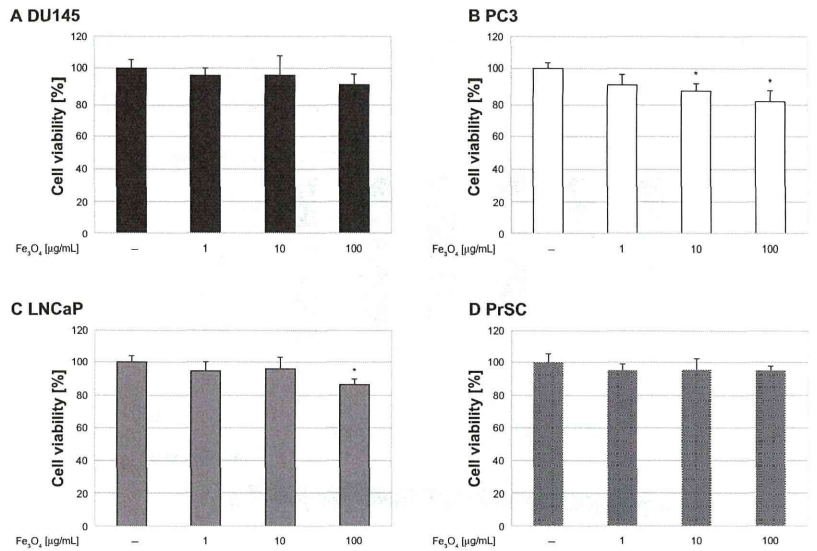

Figure 5 Effect of MgNPs-Fe_3O_4 exposure on cell line viability. Effect of MgNPs-Fe_3O_4 exposure on the viability of (**A**) DU145, (**B**) PC-3, (**C**) LNCaP, and (**D**) PrSC cell lines.
Notes: Data are presented as the mean ± SD of three independent experiments. *Significantly different from the control at $P < 0.05$.
Abbreviations: MgNPs-Fe_3O_4, Fe_3O_4 magnetic nanoparticles; SD, standard deviation.

Neither MgNPs-Fe_3O_4 nor DTX alone increased Annexin V/PI staining (Figure 8). Conversely, a significant increase in the percentage of apoptotic cells was observed during the combined treatment with NPs-Fe_3O_4 and DTX compared to the untreatment, the treatment with MgNPs-Fe_3O_4 alone, or DTX alone ($P < 0.05$).

Effect of MgNPs-Fe_3O_4 and MgNPs-Fe_3O_4–DTX combinations on NFκB expression in DU145 cells

Treatment with MgNPs-Fe_3O_4 alone did not lower NFκB expression in DU145 cells; conversely, treatment with MgNPs-Fe_3O_4–DTX combinations inhibited NFκB expression in a dose-dependent manner (Figure 9).

Discussion

DTX remains the cornerstone of chemotherapy for treating prostate cancer when castration resistance is documented and secondary hormone therapy is ineffective. However, to be effective, DTX must be administered at such high doses that can induce significant toxicity.[9,17] To overcome this drawback, combination therapies have been developed; DTX combined with tyrosine kinase or bcl-2 inhibitors are currently in Phase II studies for treating CRPC.[17] Drug-delivery assemblies consisting of a nanocarrier, a targeting agent, and DTX have also been developed. For example, NC-6301 – a polymeric micelle with DTX – shows less toxicity than native DTX in vivo; NC-6301 is a nanoscale drug delivery system approximately 100 nm in a diameter.[18] In the present study, we found that DTX alone has a strong anticancer effect, and the cytotoxic effect of a low concentration (1 nM) is augmented by MgNPs-Fe_3O_4.

Many studies have focused on the use of NPs, especially MgNPs, in theranostics.[10,11] Due to their biocompatibility and stability, iron oxide MgNPs, particularly magnetic Fe_3O_4 and its oxidized and more stable form, maghemite γ-Fe_2O_3, are superior for biomedical applications compared to other metal oxide NPs. Moreover, iron oxide NPs may have additional utility as a contrast agent in magnetic resonance imaging or as a carrier for drug delivery.[11–15] In the present study, we focused on MgNPs-Fe_3O_4 because of their potential to treat CRPC. This stems from the intrinsic properties of the magnetic core combined with the drug

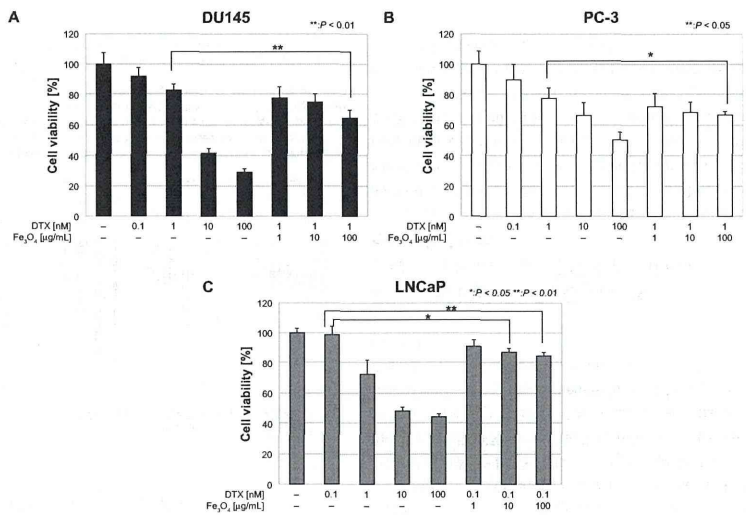

Figure 6 Effect of DTX alone or in combination with MgNPs-Fe_3O_4 on cell viability. Effect of DTX alone or in combination with MgNPs-Fe_3O_4 on the viability of (**A**) DU145, (**B**) PC-3, and (**C**) LNCaP cell lines.
Notes: Data are presented as the mean ± SD of three independent experiments. *Significantly different from the control at $P < 0.05$; **significantly different from the control at $P < 0.01$.
Abbreviations: DTX, docetaxel; MgNPs-Fe_3O_4, Fe_3O_4 magnetic nanoparticles; SD, standard deviation.

loading capability and the biomedical properties of MgNPs conferred by different surface coatings. Iron oxide MgNPs have also effectively been used in combination with chemotherapy and hyperthermia to overcome drug resistance in a leukemia xenograft model,[19] and with doxorubicin under a static magnetic field to enhance the doxorubicin-mediated cytotoxicity of MCF-7 cells.[20]

Results from several studies suggest that the cytotoxic effects of MgNPs are dependent on the metal and target cell type.[21,22] CuO, ZnO, and $CuZnFe_2O_4$, but not Fe_2O_3 or

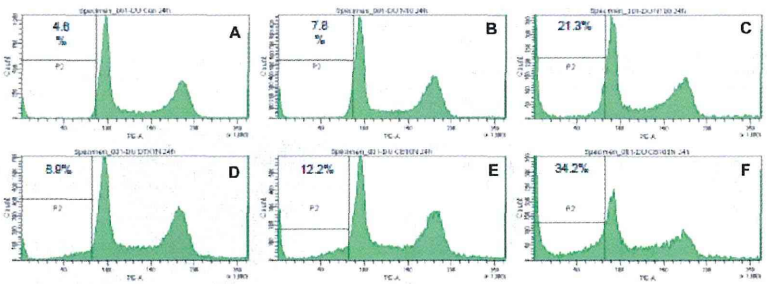

Figure 7 Flow cytometry analysis of apoptosis of DU145 cells. Panels represent the following treatments: (**A**) untreated (control); (**B**) MgNPs-Fe_3O_4 (10 µg/mL); (**C**) MgNPs-Fe_3O_4 (100 µg/mL); (**D**) DTX (1 nM); (**E**) DTX (1 nM) + MgNPs-Fe_3O_4 (10 µg/mL); and (**F**) DTX (1 nM) + MgNPs-Fe_3O_4 (100 µg/mL).
Notes: Cells were incubated with each condition for 24 hours. The percentage of cells in the sub-G1 phase was quantified for each plot.
Abbreviations: MgNPs-Fe_3O_4, Fe_3O_4 magnetic nanoparticles; DTX, docetaxel.

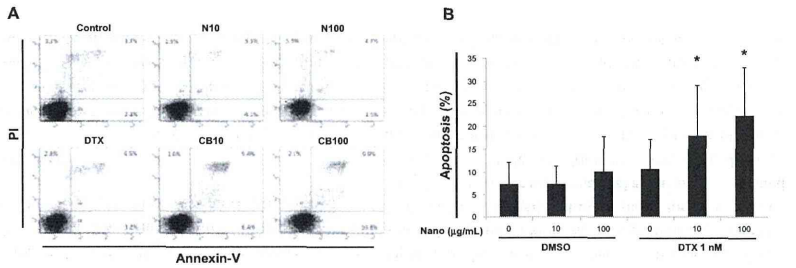

Figure 8 *Effects of MgNPs-Fe_3O_4 and docetaxel (DTX) alone or in combination on apoptosis in DU145 cells.* (**A**) *Representative FCM using Annexin V/PI staining of one set* of triplicate experiments. N10: MgNPs-Fe_3O_4 (10 µg/mL); N100: MgNPs-Fe_3O_4 (100 µg/mL); DTX: DTX (1 nM); CB10: DTX (1 nM) + MgNPs-Fe_3O_4 (10 µg/mL); and CB100: DTX (1 nM) + MgNPs-Fe_3O_4 (100 µg/mL). (**B**) Percentages of apoptotic cells from FCM analysis.
Notes: Data are presented as the mean ± SD of three independent experiments. Results show that the combination of 10 µg/mL or 100 µg/mL of MgNPs-Fe_3O_4 with 1 nM of DTX induced significant apoptosis in DU145 cells compared to untreated cells, cells treated with 10 µg/mL or 100 µg/mL of MgNPs-Fe_3O_4 alone, or 1nM of DTX alone (*$P < 0.05$).
Abbreviations: MgNPs-Fe_3O_4, Fe_3O_4 magnetic nanoparticles; DTX, docetaxel; PI, propidium iodide; DMSO, dimethyl sulfoxide; FCM, flow cytometry analysis; SD, standard deviation.

Fe_3O_4, were highly toxic to the human lung epithelial cell line A549; CuO NPs were especially effective in inducing a significant increase in ROS production.[21] In BRL 3A liver cells, only silver NPs were highly toxic; Fe_3O_4, tungsten, aluminum, and MnO_2 exhibited little or no toxicity.[23] Conversely, iron oxide MgNPs caused hepatic and renal damage when administered to mice,[22] and the reduced viability of J774 macrophages in vitro.[24]

ROS act as a second messenger in cell signaling and are involved in various biological processes, such as growth and survival in normal cells. Oxidative stress reflects a redox imbalance within the cells and usually results from

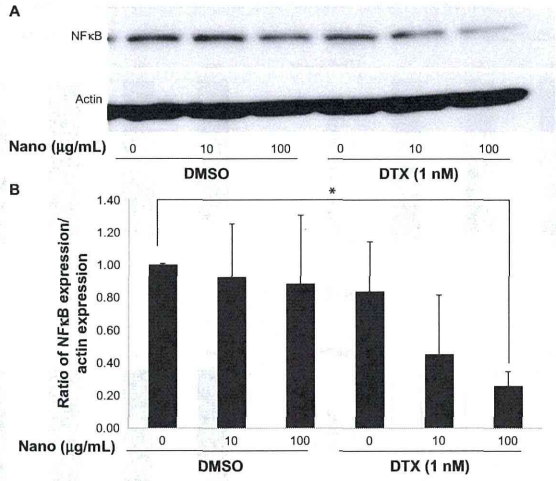

Figure 9 Effects of MgNPs-Fe_3O_4 in the absence or presence of DTX on NFκB expression in DU145 cells. (**A**) Western blot analysis. (**B**) Densitometric analysis of NFkB/ actin expression ratio.
Notes: Cells were treated for 48 hours. The ratio of NFkB expression/actin expression represents the mean ± SD of three independent experiments. Results show that NFkB expression decreased in DU145 cells treated with 100 µg/mL of MgNPs-Fe_3O_4 with 1 nM of DTX compared to untreated cells (*$P < 0.05$).
Abbreviations: MgNPs-Fe_3O_4, Fe_3O_4 magnetic nanoparticles; DMSO, dimethyl sulfoxide; DTX, docetaxel; NFκB, nuclear factor κB; SD, standard deviation.

the net accumulation of intracellular ROS, which are not detoxified by cellular antioxidative agents.[25] In cancer cells, the production of ROS is typically increased; since they play important roles in initiation, progression, and metastasis, ROS are considered oncogenic. However, ROS are also implicated in triggering cell death, including that of cancer cells; thus, their production is desirable in chemotherapy, radiotherapy, and photodynamic therapy. This dual role of ROS has led to the development of two paradoxical ROS-manipulation strategies in cancer treatment.[25] One strategy is to treat tumor cells with antioxidants, such as through the dietary administration of red wine and green tea polyphenols to prevent cancer. The other strategy is to provide pro-oxidant therapy, which consists of generating ROS directly and inhibiting antioxidative enzyme systems in tumor cells. In the present study, MgNPs-Fe_3O_4 exhibited mild cytotoxicity toward PC-3 and LNCaP, but not toward DU145 and PrSC cells. The LNCaP and PC-3 cell lines have previously been reported to have unique redox state properties, including the production of different levels of oxidative damage products and antioxidant proteins; these differences may provide new insights into the possible uses and dangers of using pro-oxidants or antioxidants as cancer therapeutic agents.[26–28] We found that the MgNPs-Fe_3O_4-induced increase in ROS was most robust in the DU145 and PC-3 cell lines; however, the levels of 8-OH-dG, an index of oxidative DNA damage, were comparably elevated in all three cell lines.

The transcription of antiapoptotic genes is activated by the NFκB signaling pathway, resulting in cell survival. The NFκB signaling pathway also plays a critical role in cancer development and progression, and in the development of tumor resistance to chemotherapy and radiation therapy,[29] particularly in the transition toward CRPC.[30] Previous studies demonstrating a relationship between elevated NFκB and a worse prognosis support this notion.[31,32] Thus, the NFκB pathway has become an important target in the development of novel anticancer treatments. The combination of magnetic NPs with either adriamycin or daunorubicin has been reported to increase p53 levels and decrease NFκB protein levels, leading to increased apoptosis in Raji lymphoma cells.[33] In the present study, treatment with MgNPs-Fe_3O_4 or DTX alone had no effect on the expression of NFκB in DU145 cells; however, treatment with MgNPs-Fe_3O_4–DTX combinations decreased expression in a dose-dependent manner. This result is unique because many NPs have been reported to activate the NFκB pathway via activation of mitogen-activated protein kinase cascades by an oxidative stress response.[34] Thus, our results suggest that the decrease in NFκB expression resulting from treatment with MgNPs-Fe_3O_4–DTX combinations may be uncoupled from ROS generation. Although the chemical components involved in NFκB inhibition and ROS production have been identified, the contribution of MgNPs-Fe_3O_4 exposure to the mechanisms of induction and action remains unclear. Further studies such as those measuring NFκB DNA-binding activity are needed.

Conclusion

We found that MgNPs-Fe_3O_4 significantly increased ROS production in prostate cancer cell lines and induced oxidative DNA damage; the cytotoxic effects of MgNPs-Fe_3O_4 alone were mild. Treatment with a combination of MgNPs-Fe_3O_4 and a low dose of DTX enhanced the inhibitory effect of DTX alone on prostate cancer cell growth in vitro, and also suppressed NFκB expression. These findings offer the possibility that MgNPs-Fe_3O_4 may allow the dose of DTX to be reduced without decreasing its antitumor activity.

Acknowledgments

We thank Dr T Yabana for TEM analysis, and Dr M Yoneda for his pathological preparation. This research was supported in part by a Grant-in-Aid for the Global COE Program from the Ministry of Education, Culture, Sports, Science and Technology of Japan, a Grant-in-Aid for Research on Risk of Chemical Substances from the Ministry of Health, Labor and Welfare of Japan, and a Research Grant-in-Aid from Magnetic Health Science Foundation.

Disclosure

The authors report no conflicts of interest in this work. The authors have no financial interests in or financial conflict with the subject matter discussed in this manuscript.

References

1. Jemal A, Siegel R, Xu J, Ward E. Cancer statistics, 2010. *CA Cancer J Clin*. 2010;60(5):277–300.
2. Tabata N, Ohno Y, Matsui R, et al. Partial cancer prevalence in Japan up to 2020: estimates based on incidence and survival data from population-based cancer registries. *Jpn J Clin Oncol*. 2008;38(2):146–157.
3. So A, Gleave M, Hurtado-Col A, Nelson C. Mechanisms of the development of androgen independence in prostate cancer. *World J Urol*. 2005;23(1):1–9.
4. Diaz M, Patterson SG. Management of androgen-independent prostate cancer. *Cancer Control*. 2004;11(6):364–373.
5. Lassi K, Dawson NA. Update on castrate-resistant prostate cancer: 2010. *Curr Opin Oncol*. 2010;22(3):263–267.
6. Tannock IF, de Wit R, Berry WR, et al; for TAX 327 Investigators. Docetaxel plus prednisone or mitoxantrone plus prednisone for advanced prostate cancer. *N Engl J Med*. 2004;351(15):1502–1512.

7. Petrylak DP, Tangen CM, Hussain MH, et al. Docetaxel and estramustine compared with mitoxantrone and prednisone for advanced refractory prostate cancer. *N Engl J Med*. 2004;351(15):1513–1520.
8. Niraula S, Tannock IF. Broadening horizons in medical management of prostate cancer. *Acta Oncol*. 2011;50 Suppl 1:141–147.
9. Lee SY, Cho JS, Yuk DY, et al. Obovatol enhances docetaxel-induced prostate and colon cancer cell death through inactivation of nuclear transcription factor-kappaB. *J Pharmacol Sci*. 2009;111(2):124–136.
10. Misra R, Acharya S, Sahoo SK. Cancer nanotechnology: application of nanotechnology in cancer therapy. *Drug Discov Today*. 2010; 15(19–20):842–850.
11. Shubayev VI, Pisanic TR 2nd, Jin S. Magnetic nanoparticles for theragnostics. *Adv Drug Deliv Rev*. 2009;61(6):467–477.
12. Cheng J, Wu W, Chen BA, et al. Effect of magnetic nanoparticles of Fe3O4 and 5-bromotetrandrine on reversal of multidrug resistance in K562/A02 leukemic cells. *Int J Nanomedicine*. 2009;4:209–216.
13. Wang C, Zhang H, Chen B, Yin H, Wang W. Study of the enhanced anticancer efficacy of gambogic acid on Capan-1 pancreatic cancer cells when mediated via magnetic Fe3O4 nanoparticles. *Int J Nanomedicine*. 2011;6:1929–1935.
14. Zhang G, Ding L, Renegar R, et al. Hydroxycamptothecin-loaded Fe3O4 nanoparticles induce human lung cancer cell apoptosis through caspase-8 pathway activation and disrupt tight junctions. *Cancer Sci*. 2011;102(6):1216–1222.
15. Sato A, Tamura Y, Sato N, et al. Melanoma-targeted chemo-thermo-immuno (CTI)-therapy using N-propionyl-4-S-cysteaminylphenol-magnetite nanoparticles elicits CTL response via heat shock protein-peptide complex release. *Cancer Sci*. 2010;101(9): 1939–1946.
16. Kawai K, Li YS, Kasai H. Accurate measurement of 8-OH-dG and 8-OH-Gua in mouse DNA, urine and serum: effects of X-ray irradiation. *Genes and Environment*. 2007;29(3):107–114.
17. Galsky MD, Vogelzang NJ. Docetaxel-based combination therapy for castration-resistant prostate cancer. *Ann Oncol*. 2010;21(11): 2135–2144.
18. Harada M, Iwata C, Saito H, et al. NC-6301, a polymeric micelle rationally optimized for effective release of docetaxel, is potent but is less toxic than native docetaxel in vivo. *Int J Nanomedicine*. 2012;7: 2713–2727.
19. Ren Y, Zhang H, Chen B, et al. Multifunctional magnetic Fe3O4 nanoparticles combined with chemotherapy and hyperthermia to overcome multidrug resistance. *Int J Nanomedicine*. 2012;7:2261–2269.
20. Aljarrah K, Mhaidat NM, Al-Akhras MA, et al. Magnetic nanoparticles sensitize MCF-7 breast cancer cells to doxorubicin-induced apoptosis. *World J Surg Oncol*. 2012;10:62.
21. Karlsson HL, Cronholm P, Gustafsson J, Möller L. Copper oxide nanoparticles are highly toxic: a comparison between metal oxide nanoparticles and carbon nanotubes. *Chem Res Toxicol*. 2008;21(9):1726–1732.
22. Ma P, Luo Q, Chen J, et al. Intraperitoneal injection of magnetic Fe3O4-nanoparticle induces hepatic and renal tissue injury via oxidative stress in mice. *Int J Nanomedicine*. 2012;7:4809–4818.
23. Hussain SM, Hess KL, Gearhart JM, Geiss KT, Schlager JJ. In vitro toxicity of nanoparticles in BRL 3A rat liver cells. *Toxicol In Vitro*. 2005;19(7):975–983.
24. Naqvi S, Samim M, Abdin M, et al. Concentration-dependent toxicity of iron oxide nanoparticles mediated by increased oxidative stress. *Int J Nanomedicine*. 2010;5:983–989.
25. Wang J, Yi J. Cancer cell killing via ROS: to increase or decrease, that is the question. *Cancer Biol Ther*. 2008;7(12):1875–1884.
26. Chen Y, Wang J, Fraig MM, et al. Defects of DNA mismatch repair in human prostate cancer. *Cancer Res*. 2001;61(10):4112–4121.
27. Trzeciak AR, Nyaga SG, Jaruga P, Lohani A, Dizdaroglu M, Evans MK. Cellular repair of oxidatively induced DNA base lesions is defective in prostate cancer cell lines, PC-3 and DU-145. *Carcinogenesis*. 2004;25(8):1359–1370.
28. Chaiswing L, Bourdeau-Heller JM, Zhong W, Oberley TD. Characterization of redox state of two human prostate carcinoma cell lines with different degrees of aggressiveness. *Free Radic Biol Med*. 2007; 43(2):202–215.
29. Gasparian AV, Guryanova OA, Chebotaev DV, Shishkin AA, Yemelyanov AY, Budunova IV. Targeting transcription factor NFkappaB: comparative analysis of proteasome and IKK inhibitors. *Cell Cycle*. 2009;8(10):1559–1566.
30. Jain G, Cronauer MV, Schrader M, Möller P, Marienfeld RB. NF-κB signaling in prostate cancer: a promising therapeutic target? *World J Urol*. 2012;30(3):303–310.
31. Koumakpayi IH, Le Page C, Mes-Masson AM, Saad F. Hierarchical clustering of immunohistochemical analysis of the activated ErbB/PI3K/Akt/NF-kappaB signalling pathway and prognostic significance in prostate cancer. *Br J Cancer*. 2010;102(7):1163–1173.
32. MacKenzie L, McCall P, Hatziieremia S, et al. Nuclear factor κB predicts poor outcome in patients with hormone-naive prostate cancer with high nuclear androgen receptor. *Hum Pathol*. 2012;43(9):1491–1500.
33. Jing H, Wang J, Yang P, Ke X, Xia G, Chen B. Magnetic Fe3O4 nanoparticles and chemotherapy agents interact synergistically to induce apoptosis in lymphoma cells. *Int J Nanomedicine*. 2010;5:999–1004.
34. Marano F, Hussain S, Rodrigues-Lima F, Baeza-Squiban A, Boland S. Nanoparticles: molecular targets and cell signalling. *Arch Toxicol*. 2011;85(7):733–741.

Int. J. Mol. Sci. **2013**, *14*, 15546-15560; doi:10.3390/ijms140815546

OPEN ACCESS
International Journal of
Molecular Sciences
ISSN 1422-0067
www.mdpi.com/journal/ijms

Article

Effects of Fe_3O_4 Magnetic Nanoparticles on A549 Cells

Masatoshi Watanabe [1,*], Misao Yoneda [2], Ayaka Morohashi [1], Yasuki Hori [1], Daiki Okamoto [1], Akiko Sato [1], Daisuke Kurioka [1], Tadashi Nittami [1], Yoshifumi Hirokawa [2], Taizo Shiraishi [2], Kazuaki Kawai [3], Hiroshi Kasai [3] and Yukari Totsuka [4]

[1] Laboratory for Medical Engineering, Division of Materials and Chemical Engineering, Graduate School of Engineering, Yokohama National University, Yokohama 240-8501, Japan; E-Mails: qqqmoro@gmail.com (A.M.); c17cssbos@gmail.com (Y.H.); dokamoto615@yahoo.co.jp (D.O.); akko.613@gmail.com (A.S.); kuri321@gmail.com (D.K.); nittami@ynu.ac.jp (T.N.)

[2] Department of Pathologic Oncology, Institute of Molecular and Experimental Medicine, Mie University Graduate School of Medicine, Tsu 514-8507, Japan; E-Mails: xyxfp209@yahoo.co.jp (M.Y.); ultray2k@clin.medic.mie-u.ac.jp (Y.H.); tao@doc.medic.mie-u.ac.jp (T.S.)

[3] Department of Environmental Oncology, Institute of Individual Ecological Sciences, University of Occupational and Environmental Health, Kitakyushu 807-8555, Japan; E-Mails: kkawai@med.uoeh-u.ac.jp (K.K.); h-kasai@med.uoeh-u.ac.jp (H.K.)

[4] Division of Cancer Development System, National Cancer Center Research Institute, Tokyo 104-0045, Japan; E-Mail: ytotsuka@gan2.res.ncc.go.jp

* Author to whom correspondence should be addressed; E-Mail: mawata@ynu.ac.jp; Tel./Fax: +81-45-339-3997.

Received: 8 June 2013; in revised form: 8 July 2013 / Accepted: 18 July 2013 / Published: 25 July 2013

Abstract: Fe_3O_4 magnetic nanoparticles (MgNPs-Fe_3O_4) are widely used in medical applications, including magnetic resonance imaging, drug delivery, and in hyperthermia. However, the same properties that aid their utility in the clinic may potentially induce toxicity. Therefore, the purpose of this study was to investigate the cytotoxicity and genotoxicity of MgNPs-Fe_3O_4 in A549 human lung epithelial cells. MgNPs-Fe_3O_4 caused cell membrane damage, as assessed by the release of lactate dehydrogenase (LDH), only at a high concentration (100 μg/mL); a lower concentration (10 μg/mL) increased the production of reactive oxygen species, increased oxidative damage to DNA, and decreased the level of reduced glutathione. MgNPs-Fe_3O_4 caused a dose-dependent increase in the $CD44^+$ fraction of A549 cells. MgNPs-Fe_3O_4 induced the expression of heme oxygenase-1 at a concentration of 1 μg/mL, and in a dose-dependent manner. Despite these effects, MgNPs-Fe_3O_4 had minimal effect on cell viability and elicited only a small increase in the number of cells undergoing apoptosis. Together, these data suggest that MgNPs-Fe_3O_4 exert little or no cytotoxicity until a high exposure level (100 μg/mL) is reached. This dissociation between elevated indices of cell damage and a small effect on cell viability warrants further study.

Keywords: magnetic nanoparticles; cytotoxicity; genotoxicity; A549; CD44

1. Introduction

Nanotechnology—the manipulation and production of matter sized between 1 and 100 nm—has grown markedly with the promise of substantial benefits and applicability to such diverse areas as clothing, electronics, engineering, and healthcare [1]. The principal goal of nanotechnology is to develop new materials in the nanometer scale, including nanoparticles, defined as particulate materials with at least one dimension of less than 100 nm. The design and development of nanomaterials have been of fundamental importance to the industry, given their novelty and the benefits conferred by their physicochemical properties.

Magnetic nanoparticles (MgNPs) are a subclass of nanomaterials. Among MgNPs, Fe_3O_4-containing MgNPs (MgNP-Fe_3O_4; magnetite) are the only MgNPs approved for clinical use. Magnetite has a cubic inverse spinel structure with oxygen forming a face-centered cubic (FCC) closed packing; the interstitial tetrahedral and octahedral sites are occupied by Fe cations [2]. Due to their unique physical, chemical, and mechanical features, MgNPs-Fe_3O_4 have been used as magnetic resonance imaging contrast agents, targeted drug delivery systems, and hyperthermic agents when placed in an external magnetic field [3,4]. Modified/unmodified MgNP-Fe_3O_4 has been reported to improve the efficiency of anticancer drugs and reverse multidrug resistance [5,6]. However, these same properties of MgNPs can induce cytotoxicity and genotoxicity [7]. Studies have shown that MgNPs-Fe_3O_4 are less toxic than MgNPs containing SiO_2, TiO_2, CuO, and TiO_2 [7–9]. However, results regarding the potential of MgNPs-Fe_3O_4 to induce cytotoxicity, genotoxicity, and oxidative stress, have been inconsistent [7–11], necessitating further study to identify any potential toxicity associated with their use. Therefore, the objective of this study was to investigate the cytotoxicity and genotoxicity of MgNPs-Fe_3O_4. Experiments were designed to examine the effect of MgNPs-Fe_3O_4 on indices of oxidative stress, and resultant cellular and nuclear damage in A549, human alveolar epithelial-like type-II cells. We also assessed the effect of MgNPs-Fe_3O_4 on the expression of CD44, a transmembrane glycoprotein involved in inflammation, cell migration, signaling, and tumor metastasis [12,13].

2. Results and Discussion

Studies regarding the toxicological impact of MgNPs-Fe_3O_4 have yielded disparate results, depending on the cell type, surface modification, cell medium composition, protein-MgNP interaction,

and oxidation state of iron [7,14]. We evaluated the cytotoxic effects of MgNPs-Fe_3O_4 in A549 cells. We report that MgNPs-Fe_3O_4 caused LDH leakage only at a concentration of 100 μg/mL; increased ROS production and 8-OH-dG content, and decreased glutathione (GSH) levels were found with 10 μg/mL MgNPs-Fe_3O_4. Despite these responses, MgNPs-Fe_3O_4 caused only a small decrease and increase in cell viability and apoptosis, respectively.

Figure 1. Measurement of MgNPs-Fe_3O_4 size by dynamic light scattering. MgNPs-Fe_3O_4 were suspended at a concentration of 1, 10 or 100 μg/mL in (**a**) Ham's F-12 Medium with 10% fetal bovine serum (FBS); (**b**) Ham's F-12 Medium alone; (**c**) Phosphate-buffered saline (PBS).

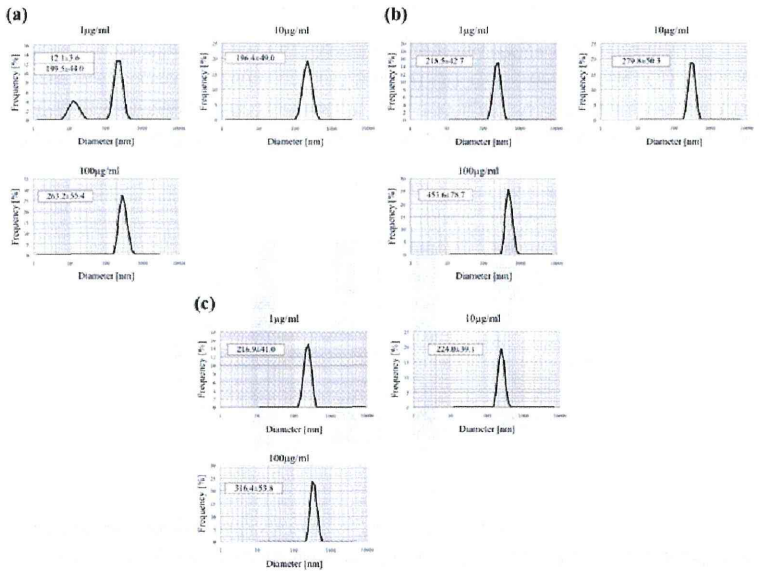

2.1. Characterization of MgNPs-Fe_3O_4 Suspension in Various Conditioned Medium

One of the most important significant factors for analysis of the toxicity of nanoparticles is size. As well as the sizes of the primary nanoparticles, the hydrodynamic sizes of secondary nanoparticles in dispersion are important as their sizes have a dramatic effect on cell response to exposure. The high ionic nature of the solution and the electrostatic/van der Waals interaction between protein and nanoparticles results in the formation of secondary particles. The mean hydrodynamic diameter of MgNPs-Fe_3O_4 in Ham's F-12 medium, without FBS or supplements, increased in a dose-dependent manner (Figure 1b). In Ham's F-12 medium with 10% FBS and supplements or PBS, the mean hydrodynamic diameter was comparable between MgNP-Fe_3O_4 suspensions of 1 and 10 μg/mL (Figure 1a,c); mean hydrodynamic diameter of MgNPs-Fe_3O_4 was greater at 100 μg/mL in both media.

Together, these data suggest that MgNPs-Fe_3O_4 agglomerate at a high concentration. The presence of FBS appeared to enhance the stability of MgNPs-Fe_3O_4 in suspension. These data are consistent with a previous report showing that MgNPs show increased stability against aggregation in the RPMI-1640 with an increasing amount of FBS [15]. Therefore, the influence by the sedimentation rate of the secondary nanoparticles (NPs) and rations of protein to NPs could be taken into consideration in the *in vitro* toxicity of NPs. These results shows the hydrodynamic sizes of secondary nanoparticles in Ham's F-12 medium with 10% FBS used in this study.

2.2. MgNPs-Fe_3O_4 Uptake

A representative micrograph shows that after 24 h, MgNPs-Fe_3O_4 aggregate within intracellular vesicles in A549 cells (Figure 2a). Figure 2b shows the flow cytometric light scatter histograms of the cells treated with the 0, 1, 10, or 100 μg/mL MgNPs-Fe_3O_4. The forward-scattered (FS) intensity (reflective of cell size) did not change; conversely, side-scattered (SS) intensity (reflective cellular uptake) increased in a dose-dependent manner. That is, the cells, which took up higher doses of MgNPs showed higher intensities of SS.

Figure 2. MgNPs-Fe_3O_4 uptake in A549 cells; (**a**) Transmission electron microscopy imaging of A549 cells treated with 10 μg/mL Fe_3O_4 magnetic nanoparticles (MgNPs-Fe_3O_4) for 24 h. MgNPs-Fe_3O_4 are enclosed in vesicles (arrow); (**b**) Analysis of MgNPs-Fe_3O_4 uptake by flow cytometric light scatter. A549 cells were treated with 0 (control), 1, 10 or 100 μg/mL MgNPs-Fe_3O_4 for 24 h. SS: side-scattered; FS: forward-scattered.